21st Australasian Fluid Mechanics Conference
Adelaide, Australia
10-13 December 2018

Application of Discontinuous Galerkin Methods for Fluid Thermal Structure Interaction Problems

Z.Cai[1] and B.Thornber[2]

[1,2]School of Aerospace, Mechanical and Mechatronic Engineering
University of Sydney, NSW, Australia

Abstract

The principle benefit of using the discontinuous Galerkin (DG) methods is that they can produce a high order accurate scheme which can achieve an equivalent error compared to the lower order scheme with orders of magnitude lower computational effort. Furthermore, DG methods have a built-in stabilisation mechanism when solving problems with complex geometry which make it highly suitable to be implemented in fluid-structure interactions problems. This paper presents a framework for the computation of fluid thermal structure interaction problems within a single domain using DG methods on unstructured grids. The full solver consists of four main components: an incompressible fluid solver, a conjugate heat transfer (CHT) solver, a linear elastic solver and a fluid to structure interaction (FSI) coupling. Based on an existing DG solver for the incompressible Navier-Stokes (INS) equation, the fluid advection-diffusion equation, the Boussinesq term, the solid heat equation and the linear elastic equation are introduced using an explicit DG formulation. A Dirichlet-Neumann partitioning strategy has been implemented to achieve the data exchange process via the numerical flux of interface quadrature points in the fluid-solid interface. Formal h and p convergence studies employing the method of manufactured solutions (MMS) demonstrate that the expected order of accuracy is achieved. The algorithm is then further validated against the lid-driven cavity with a flexible bottom wall. The DG results show good agreement with the benchmark data and the h and p convergence tests demonstrate clearly that very high-order methods use substantially lower computational time for equivalent error norms when compared to second order approaches.

Introduction

In fluid to structure interaction (FSI) problems, solid structure interacts with internal or external fluid flow. The numerical procedures to solve the FSI problems can be broadly classified into two approaches:(i) monolithic approach and (ii) partitioned approach. The monolithic approach treats the fluid and structure dynamics in the same mathematical frameworks to form a single system equation for the entire problem, which is solved simultaneously by a unified algorithm. This approach can potentially achieve better accuracy for a multidisciplinary problem, but it may require more resources and expertise to develop and maintain such a specialised code. On the other side, the partitioned approach treats the fluid and the structure as two computational fields which can be solved separately with their respective mesh discretisation and numerical algorithm. The information between the fluid and solid are exchanged as interfacial conditions on the interaction face. The partitioned approach can take advantage of existing codes for solving many complex fluid and structure problems.

Discontinuous Galerkin (DG) methods belong to the class of finite elements. The finite element function space corresponding to DG methods consists of piecewise polynomials which can be completely discontinuous across element interfaces. The first DG method was introduced by Reed and Hill [5] to solve the steady-state neutron transport equation. The DG method has many beneficial features, such as the potential for high-order scalability and stability for complicated geometries. These key features help to make FSI modellng more accurate, and robust compared to the traditional finite element method. However, before these positive gains can be realized, a formulation for a loose-coupled FSI problem must be demonstrated using the DG method.

The early research of using the DG approach to solve FSI problems date back to 2009. Nguyen developed a numerical method for simulations of flow over variable geometries including deformable domains or moving boundaries by a high-order DG method in the framework of an Arbitrary Lagrangian Eulerian (ALE) approach to take into account the deformable domains [2]. Froehle and Persson [3] extended the FSI problem to the compressible flow where different methods were implemented in the fluid and the solid domain. The fluid is discretised using a DG method on unstructured tetrahedral meshes, and the structure uses a high-order volumetric continuous Galerkin finite element method. Recently Sheldon and Mille presented the application of the hybrid discontinuous Galerkin (HDG) method to the multi-physics simulation of coupled FSI problems [4]. The elasticity formulations are written in a Lagrangian reference frame, with the nonlinear formulation restricted to hyper-elastic materials.

The primary motivation of this paper is to present accurate, high-order viscous computations of fluid-thermal-structural interaction between the solid domains with a steady-state incompressible flow. The governing equations are the incompressible Navier-Stokes equations, complemented by an additional advection-diffusion equation that is used to determine the fluid temperature, the Boussinesq term to calculate the impact of gravity, the solid heat equation to determine the temperature in the solid domain and an additional solid linear elastic equation to determine the solid displacement. All the modelling equations are solved using the DG methods as the basic equations. The manufactured solution approach and one benchmarks case are presented to validate the implementation of all key governing equations. All the numerical results have shown good convergence in both p and h refinement.

Governing Equation and Numerical Methods

The Boussinesq approximation is included to couple the temperature and flow field for the fluid domain. The governing equations for steady-state two-dimensional flow on a generalised coordinate system using the Incompressible Navier-Stokes (INS) equations and advection-diffusion equation can be written with the following dimensionless variables:

$$\nabla \cdot \mathbf{U}_f = 0, \tag{1}$$

$$\mathbf{U}_f \cdot \nabla \mathbf{U}_f = -\nabla P + Pr \cdot \nabla^2 \mathbf{U}_f + \frac{g\beta L^3}{{\alpha_f}^2}(T_f - T_q), \tag{2}$$

$$\mathbf{U}_f \cdot \nabla \mathbf{T}_f = \alpha_f \nabla^2 T_f. \tag{3}$$

Where:

$$\mathbf{U}_f = [\frac{u_f}{\alpha_f}, \frac{v_f}{\alpha_f}]; P = \frac{p}{\rho_f \alpha_f^2}. \quad (4)$$

$$Pr = \frac{\nu}{\alpha_f}; \alpha_s = \frac{k_s}{(\rho Cp)_s}; \alpha_f = \frac{k_f}{(\rho Cp)_f}. \quad (5)$$

Here subscript f and s is for the fluid and solid phases respectively. X and Y are dimensionless coordinates varying along horizontal and vertical directions respectively; U_f are dimensionless velocity components in the X and Y directions; u_f and v_f are velocity components in X and Y direction respectively; T_f is the fluid temperature, ν is the kinematic viscosity; ρ_f and ρ_s are the density of solid and fluid phases respectively; k_s and k_f are thermal conductivity of solid and fluid medium respectively; $(Cp)_s$ and $(Cp)_f$ are heat capacity of solid and fluid medium respectively; α_s and α_f are thermal diffusivity in solid and fluid phases respectively; T_q is the quiescent temperature; P is the dimensionless pressure and p is the pressure; L is the characteristic length; Pr is the Prandtl number respectively.

The governing equation for the steady-state two-dimension heat equation in the solid domain is:

$$\frac{q}{(\rho Cp)_s} = \alpha_s \nabla^2 T_s. \quad (6)$$

where q is the heat generated per unit volume, α_s is the thermal diffusivity in the solid domain.

The governing equation for displacement within a solid domain for a steady-state two-dimension linear elastic problem is expressed in Navier Form as:

$$\frac{\lambda+\mu}{\rho_s}\nabla\nabla\cdot U_s + \frac{\mu}{\rho_s}\nabla^2 U_s - \frac{F}{\rho_s} - \frac{\alpha_{ts}\beta\nabla T_s}{\rho_s} = 0. \quad (7)$$

Where:

$$\mu = \frac{E}{2(1+\upsilon)}; U_s = \{u_s; v_s\}. \quad (8)$$

u_s and v_s are the displacement components in the X and Y directions; E and υ are the Young's module and Poisson ratio of the solid material respectively. α_{ts} is the thermal expansion coefficient of the material. F is the external body force. For the plain stress problem, λ and β are defined as:

$$\lambda = \frac{E\upsilon}{(1+\upsilon)(1-\upsilon)}, \beta = 2\mu\frac{3\lambda+2\mu}{\lambda+2\mu} \quad (9)$$

For plain strain problems, λ and β are defined as:

$$\lambda = \frac{E\upsilon}{(1+\upsilon)(1-2\upsilon)}, \beta = 2\mu+3\lambda \quad (10)$$

The DG discretization of the INS equation is strictly following Hesthaven's INS-DG solver [8]. The details of the DG discretization for the advection-diffusion equation,solid heat equation and linear elastic equation were presented in the former work([7] and [6]).

To conjugate the solid displacement and fluid pressure between the fluid and the solid domain, a loose-coupled Dirichlet-Neumann partitioning approach is applied to solve steady-state fluid to solid interaction problems. The fundamental conditions applied to the fluid to structure interfaces are the displacement compatibility and the traction equilibrium Eq. (11).

$$d_f = d_s; n\cdot\tau_s = n\cdot\tau_f. \quad (11)$$

The displacement of the solid domain is calculated by the linear elastic equation first. The fluid nodal positions on the fluid-structure interfaces are then determined by Eq. (11) and applied as the Dirichlet boundary condition. The displacements of the other fluid nodes are derived through the linear elastic equation within the full fluid domain. Due to mesh deformation in both the fluid and the solid domain, the grid matrix and system matrix need to be updated in each calculation step. The governing equations of fluid flow in their ALE formulations are then solved as shown in Eq. (12), following the heat equation in the solid domain. $\mathbf{U}_g$ here is the moving coordinate velocity, and $(\mathbf{U}_f - \mathbf{U}_g)$ is the relative velocity of the fluid with respect to the moving coordinate velocity.

$$\begin{aligned} \nabla\cdot\mathbf{U}_f &= 0, \\ (\mathbf{U}_f-\mathbf{U}_g)\cdot\nabla\mathbf{U}_f &= -\nabla P + Pr\cdot\nabla^2\mathbf{U}_f + + \frac{g\beta L^3}{{\alpha_f}^2}(T_f - T_q), \\ \mathbf{U}_f\cdot\nabla\mathbf{T}_f &= \alpha_f\nabla^2 T_f. \end{aligned} \quad (12)$$

In steady-state analyses, the mesh velocities are always set to zero even the fluid nodal displacements are updated. Accordingly, the fluid speeds on the fluid-structure interfaces are zero. According to the traction equilibrium conditions, the fluid traction is integrated into fluid force along fluid-structure interfaces and exerted onto the structure node as the equation shown below:

$$F_f(t) = \int h^d \tau_f \cdot dS. \quad (13)$$

where F_f is the fluid force, h^d is the virtual quantity of the solid displacement and S is the surface area near the fluid-solid interaction.

Manufactured Solution Approach and Benchmarks

Manufactured Solution Approach

The manufactured solution to validate the fluid-thermal-structural interaction solver is prescribed as follows;

In the Fluid domain:

$$\begin{aligned} u_f &= cos(x)sin(y) + sin(x)cos(y), \\ v_f &= -sin(x)cos(y) - cos(x)sin(y), \\ p &= 2\nu(sin(x)sin(y) - cos(x)cos(y)) - 6cos(x)sin(y), \\ T_f &= sin(\pi x)cos(\pi y) + 0.25cos(\pi y). \end{aligned} \quad (14)$$

In the Solid domain:

$$\begin{aligned} T_s &= \tfrac{k_f}{k_s}sin(\pi x)cos(\pi y) + 0.25cos(\pi y), \\ u_s &= 0.05sin(x)cos(y), \\ v_s &= 0.05cos(x)sin(y). \end{aligned} \quad (15)$$

Where u_f and v_f is the velocity in X and Y direction, p is the pressure in the fluid domain, T_f and T_s is the temperature in fluid domain and solid domain respectively, u_s and v_s is the solid displacement in horizontal and vertical displacement. The fluid properties are set as: $Pr = 0.5, \alpha_f = 1.0, Ra = 2.0$ while in the solid domain $\alpha_s = 1.0, E = 1.0, \upsilon = 0.3$. Please note that the solid to fluid interaction surface will deform due to the solid domain deformation. Consequently, the fluid and solid thermal

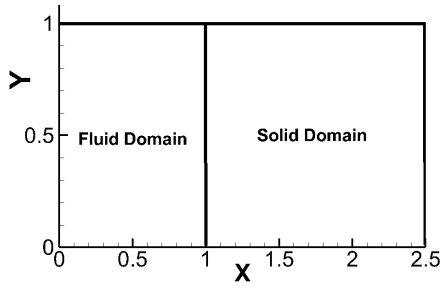

Figure 1: Domain for the manufactured solution to verify the FSI solver

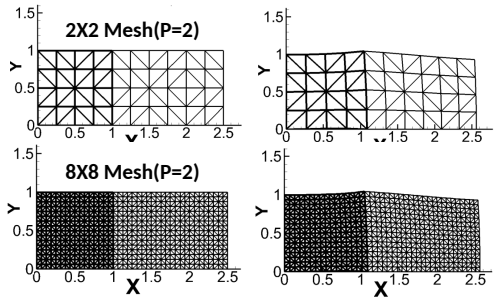

Figure 2: h-refinement meshes used for the MMS for FSI solver

diffusivity have to be forced to be same to ensure the temperature continuity on the FSI interaction interface. The Fluid is within a $[X = 0,1; Y = 0,1]$ domain while the solid is domain is within $[X = 1,2.5; Y = 0,1]$ as shown in Figure 1. Due to the natural of the MMS approach, the thermal stress in the solid domain is offset by the source term and the displacement field will convergence to the displacement field as shown in Eqt.15.

To calculate the fluid mesh deformation, the linear elastic equation is applied in the full fluid domain. The fluid elastic module and Poisson ratio are set as: $E_f = 10.0, \upsilon = 0.1$. Stress-free boundary conditions are applied as the Neumann boundary condition on the top and bottom wall of the fluid domain. The fluid mesh displacement is forced to be 0 for the edge at $x = 0$; while at each time step, the displacement calculated from the solid domain is applied as the Dirichlet boundary condition to the fluid to structure interaction edge. Three sets of meshes are used to validate the convergence speed which start from 2×2 ($h = 0.5$) to 8×8 ($h = 0.125$). The polynomial order goes up to the 3^{rd} order. The detailed mesh before and after deformation used in hp study are shown in Figure 2 and Figure 3 respectively.

The normalized $L1$ error as a function of hp refinement for horizontal velocity, vertical velocity, fluid temperature and solid

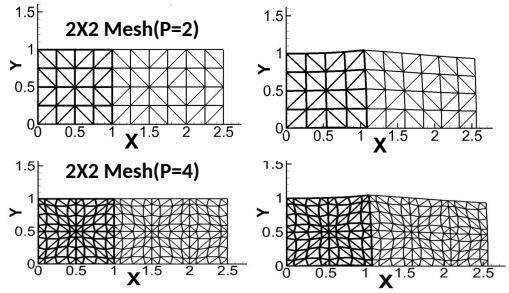

Figure 3: p-refinement meshes used for the MMS for FSI solver

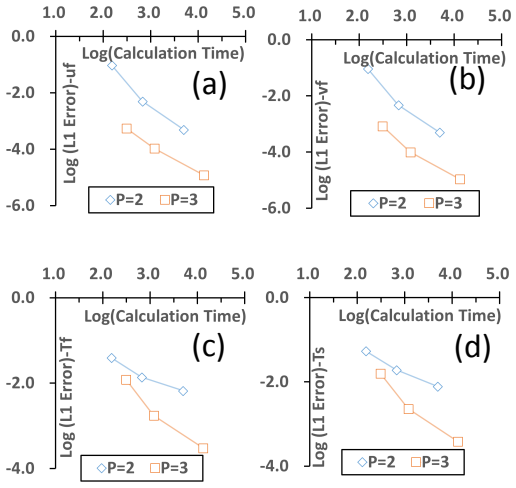

Figure 4: Normalized L_1 error versus calculation time for the FSI solver (note: log axes)(a)u_f (b)v_f (c)T_f (d)T_s

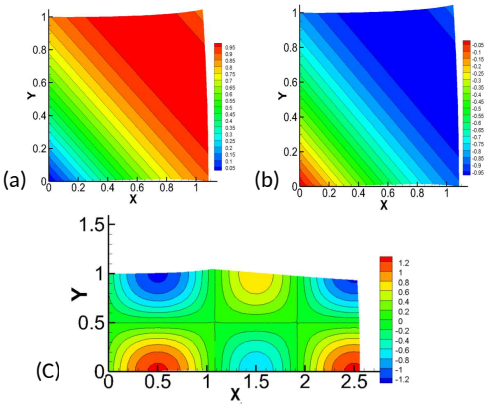

Figure 5: Contour plots of the solution to the MMS solution of the FSI solver-($8 \times 8 mesh, p = 3$)(a)u_f (b)v_f (c)T_f and T_s

temperature are plotted from Figure 4, where log-log axes are employed. These figures demonstrate clearly that the higher order accurate schemes can achieve an equivalent error to the lower order schemes with orders of magnitude lower computational effort. The contour plots of u_s,v_s,T_f and T_s are shown in Figure 5.

Benchmark-Lid-Driven Cavity with a Flexible Bottom Wall

The second test case was to validate the DG code for fluid-structure interaction problems. A two-dimensional square cavity with the physical dimensions is shown in Figure 6. The cavity is within a 1×1 domain while a $h = 0.002$ thick flexible bottom wall is attached to the bottom of the cavity. The working fluid is assumed to be an incompressible Newtonian fluid with a Prandtl number of 0.71. The top lid is assumed to move from left to right at a constant speed $U = 1$ at maintained higher temperature $T_h = 1$. Two vertical walls are assumed to be insulated while the bottom wall is fixed at the lower temperature $T_c = 0$. The Reynolds number is set to be 100, and the Grashof number equal to 100. Conduction through the flexible wall is assumed to be negligible. The left and right wall of the solid domain is fixed. The physical properties of the flexible bottom wall are assumed to be constant and homogeneous. The default values chosen for the flexible wall were as follows: density

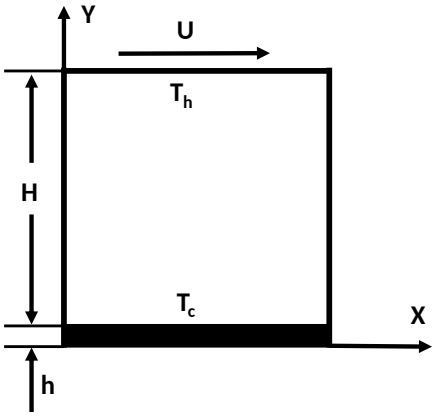

Figure 6: Configuration of the lid-driven cavity with a flexible bottom wall [9](a)u_f (b)T_f

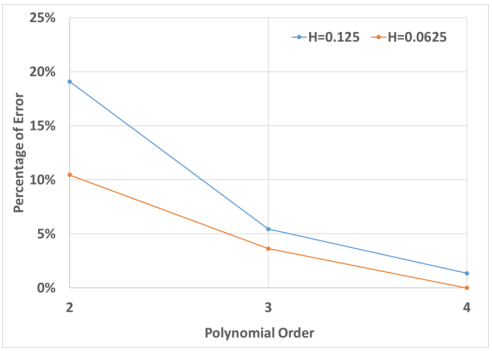

Figure 7: Convergence of the average Nusselt number at the top wall between various studies for the cavity with the flexible wall

$\rho_s = 500kg/m^3$, elastic Module $E = 25000N/m^2$ and Poisson's ratio $\upsilon = 0.45$.

To simulate the lid-driven cavity with the flexible bottom wall, uniform meshes with 8×8 to 16×16 nodes are used for the fluid domain while the solid domain is modelled using iso-parametric beam elements. The polynomial order goes up to the $4th$ order. The convergences of the average Nusselt number on the flexible wall against the posted benchmark are presented in Figure. 7. The contour plot of the streamline and T_s are shown in Figure. 8.

Conclusions

This paper presents the framework of a discontinuous Galerkin approach for steady fluid-thermal-structural interaction on unstructured meshes. The investigation is motivated by the need for accurate simulation of such problems in mechanical, aerospace and biomedical engineering applications. A loosely coupled Dirichlet-Neumann partitioning approach is proposed to couple the fluid-solid and solid-solid interfaces based on the numerical flux of quadrature points.

A single case has been proposed based on the method of manufactured solutions to validate and verify all key terms and the coupling method in all governing equations. The observed order of spatial accuracy approaches the corresponding polynomial order when the grid is defined as expected. Further benchmark cases were presented to validate the accuracy of the DG solver

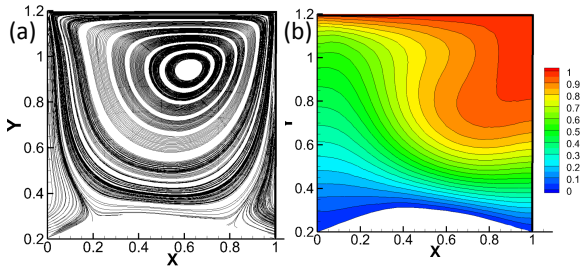

Figure 8: Contour plot for the lid-driven cavity with a flexible bottom wall (8×8 mesh, $p = 4$)(a)the streamline(b)T_f

against previously published computations. Promising convergence has been demonstrated for both h and p refinement.

This DG solver has the potential to be expanded to solve engineering-focused FSI problems. Further research will focus on developing this methodology to full laser package thermal expansion modelling and chip bending on the printed circuit board.

References

[1] Roe, B., Haselbacher, A. and Geubelle, P.H., Stability of fluid–structure thermal simulations on moving grids, *International journal for numerical methods in fluids.*, **9**, 2007, 1097–1117.

[2] Nguyen, V.T., An Arbitrary Lagrangian–Eulerian discontinuous Galerkin method for simulations of flows over variable geometries, *Journal of Fluids and Structures.*, **26**, 2010, 312–329.

[3] Froehle, B. and Persson, P.O., A high-order discontinuous Galerkin method for fluid–structure interaction with efficient implicit–explicit time stepping, *Journal of Computational Physics.*, **272**, 2014, 312–329.

[4] Sheldon, J.P., Miller, S.T. and Pitt, J.S., A hybridizable discontinuous Galerkin method for modeling fluid–structure interaction, *Journal of Computational Physics.*, **326**, 2016, 91–114.

[5] Reed, W.H. and Hill, T.R., Triangular mesh methods for the neutron transport equation, *Los Alamos Scientific Lab., N. Mex.(USA).*, 1973.

[6] Cai, Z. and Thornber, B., An investigation of the application of discontinuous Galerkin method for conjugate heat transfer of thermoelectric cooler, *20th Australasian Fluid Mechanics Conference.*, 2016.

[7] Cai, Z. and Thornber, B., An internal penalty discontinuous Galerkin method for simulating conjugate heat transfer in a closed cavity, *International Journal for Numerical Methods in Fluids.*, **87**, 2018, 134-159.

[8] Hesthaven, J.S. and Warburton, T., Nodal discontinuous Galerkin methods: algorithms, analysis, and applications, *Springer Science & Business Media.*, 2007.

[9] Al, A.A. and Khanafer, K.,Fluid–structure interaction analysis of mixed convection heat transfer in a lid-driven cavity with a flexible bottom wall, *International Journal of Heat and Mass Transfer.*, **54**, 2011, 3826-3836.